RESEARCH ARTICLE

EW-7197 eluting nano-fiber covered self-expandable metallic stent to prevent granulation tissue formation in a canine urethral model

Kichang Han[1☯‡], Jung-Hoon Park[2,3,4☯‡], Su-Geun Yang[5]*, Deok Hee Lee[2]*, Jiaywei Tsauo[2], Kun Yung Kim[2], Min Tae Kim[2], Sung Gwon Gang[2], Dae-Kee Kim[6], Dong-Hyun Kim[4], Ho-Young Song[2]

1 Department of Radiology, Severance Hospital, Research Institute of Radiological Science, Yonsei University, College of Medicine, Seoul, Republic of Korea, 2 Department of Radiology, Research Institute of Radiology, Asan Medical Center, University of Ulsan College of Medicine, Seoul, Republic of Korea, 3 Department of Biomedical Engineering Research Center, Asan Medical Center, University of Ulsan College of Medicine, Seoul, Republic of Korea, 4 Department of Radiology, Northwestern University Feinberg School of Medicine, Chicago, IL, United States of America, 5 Department of New Drug Development and WCSL, Inha University College of Medicine, Incheon, Republic of Korea, 6 College of Pharmacy, Ewha Womans University, Seoul, Republic of Korea

☯ These authors contributed equally to this work.
‡ These authors are co-first authors on this work.
* Sugeun.Yang@Inha.ac.kr (SGY); dhlee@amc.seoul.kr (DHL)

Abstract

Purpose

To evaluate an EW-7197-eluting nanofiber-covered stent (NFCS) for suppressing granulation tissue formation after stent placement in a canine urethral model.

Materials and methods

All experiments were approved by the committee of animal research. A total of 12 NFCSs were placed in the proximal and distal urethras of six dogs. Dogs were divided into two groups with 3 dogs each. The control stent (CS) group received NFCSs and the drug stent (DS) group received EW-7197 (1000 μg)-eluting NFCSs. All dogs were sacrificed 8 weeks after stent placement Histologic findings of the stented urethra were compared using the Mann-Whitney U test.

Results

Stent placement was technically successful in all dogs without procedure-related complications. On urethrographic analysis, the mean luminal diameter was significantly larger in the DS group than in the CS group at 4 and 8 weeks after stent placement (all $p < 0.001$). On histological examination, mean thicknesses of the papillary projection, thickness of submucosal fibrosis, number of epithelial layers, and degree of collagen deposition were significantly lower in the DS group than in the CS group (all $p < 0.001$), whereas the mean degree of inflammatory cell infiltration was not significantly different ($p > 0.05$).

Conclusion

The EW-7197-eluting NFCS is effective and safe for suppressing granulation tissue formation after stent placement in a canine urethral model.

Introduction

Placement of a covered self-expandable stent (SEMS) is a well-established method for the treatment of luminal strictures involving various nonvascular organs [1–5]. However, these stents exert constant mechanical stress to the adjacent tissue, resulting in granulation tissue formation. This is a major drawback of stent placement because granulation tissue formation can cause restenosis and recurrence of symptoms. Stent placement in the urethra is not an exception; therefore, granulation tissue formation is widely recognized as one of the most important obstacles to long-term stent placement in the urethra [5–8].

There is a growing understanding of the molecular mechanism of granulation tissue formation, and transforming growth factor-β1 (TGF-β1) has emerged as a key component in the proliferation of granulation tissue [9,10]. The desire to block the TGF-β1 signaling pathway has led to the development of several small-molecule drugs that act by inhibiting TGF-β1 from binding to its receptors [11,12]. Of these, EW-7197 is a novel oral TGF-β type-1 receptor kinase inhibitor [13,14]. This drug has been shown to have strong antifibrotic properties in animals [15,16] and the development of a drug-eluting stent using EW-7197 may be an attractive alternative for suppressing granulation tissue formation after stent placement in the urethra. Nanofiber meshes are flexible and highly porous meshes that is suitable for coating metallic stents and providing local drug delivery [17]. Recently, we have developed an EW-7197-eluting nanofiber-covered stent (NFCS). We hypothesized that this stent would suppress granulation tissue formation after stent placement in the urethra. Therefore, the purpose of this study was to evaluate EW-7197-eluting NFCSs for suppressing granulation tissue formation after stent placement in a canine urethral model.

Materials and methods

EW-7197-eluting nanofiber-covered stent

Stent construction. The stent used in this study was woven six times into a tubular configuration with six bends from a single thread of 0.15-mm-thick nitinol wire filament (Fig 1A). When fully expanded, the stent had a diameter of 10 mm and a length of 20 mm. Two radiopaque markers were attached to the ends of the stent to facilitate stent placement. The stent was made to our specifications by a local manufacturer (S&G biotech, Seongnam, Korea).

EW-7197-eluting nanofiber coating over the stent. The nanofiber covering membrane [drug-eluting poly-DL-lactic acid (PDLLA) and polyurethane (PU) backing layers] used in this study was constructed using electrospinning techniques. The electrospun scaffolds were constructed on the surface of the rolling stent and vacuum dried at room temperature for 24 h. PU (10 w/v%) and solvent polymer (90 w/v%) as a core was dissolved in tetrahydrofuran/dimethylacetamide (2:1) solution and then electrospun from the syringe at a rate of 0.2 ml/h. PDLLA (3.3 w/v%) and EW 7197 (20 w/v%) as a shell was sprayed from the syringe at a rate of 0.73 ml/h at the same time. The stents were rotated at 300 rpm and increased to 500 rpm over 2–4 h. Each EW-7197-eluting NFCS contained 1000 μg of EW-7197. A nanofiber layer on the surface of the stent was examined with a scanning electron microscope (SEM; TM-1000; Hitachi, Krefeld, Germany). The electrospun layer exhibited an apparent nanofiber structure, as shown in Fig 1B.
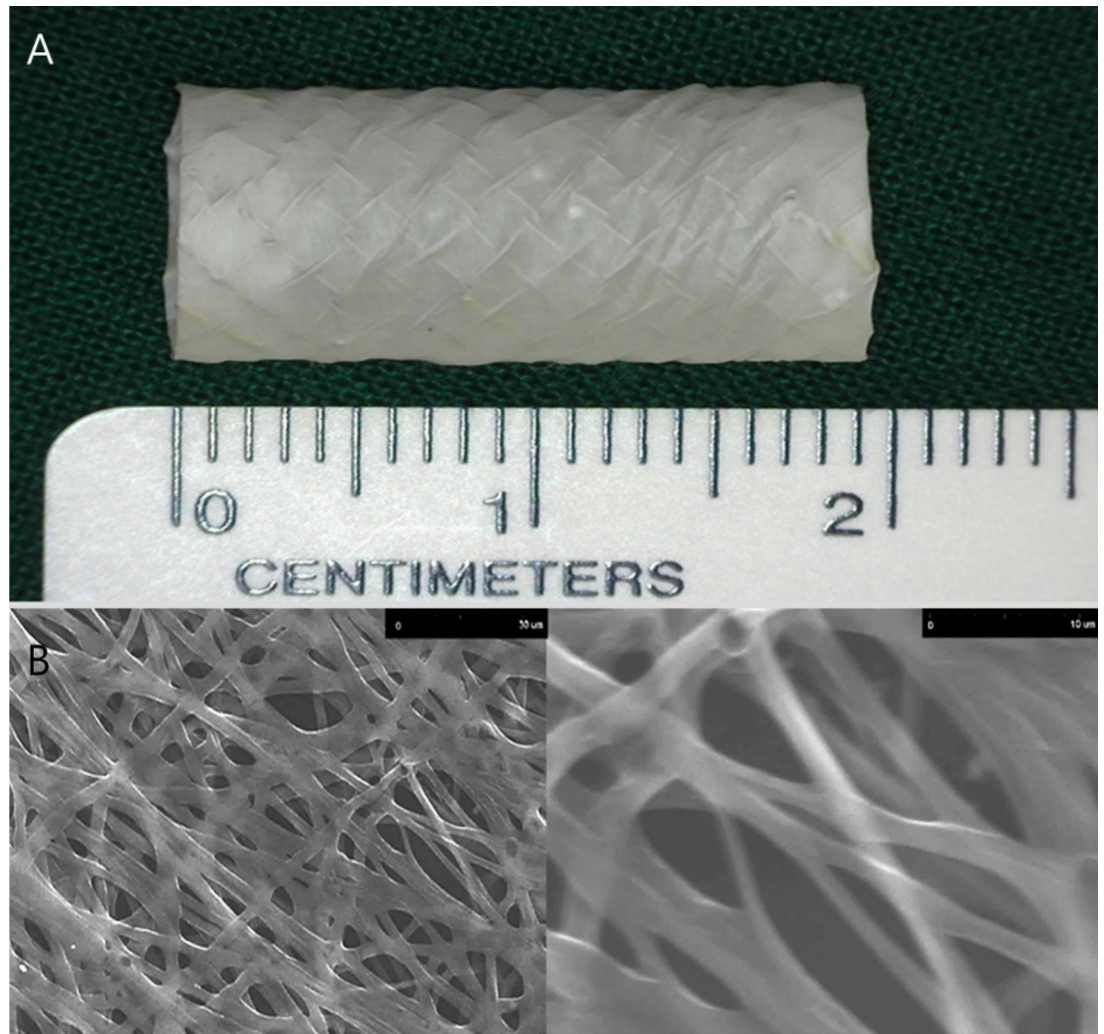
Fig 1. Representative optical images of (A) Nanofiber-covered, self-expandable metallic stent and (B) scanning electron micrographs of EW-7197 loaded nanofibers. The scale bars are 30 μm and 10 μm.

***In vitro* release study of EW-7197 nanofiber membrane.** EW-7197 nanofiber membrane was placed inside a 50-mL conical tube with 50 mL of release medium, 10-mM PBS buffer of pH of 7.4 (n = 6). The tubes were placed in a shaking incubator at 37°C and 50 rpm. The release medium in each tube was collected at the predetermined time for further analysis, replaced with fresh media, and the concentration of EW-7197 was determined using a (high performance liquid chromatography) HPLC system (Agilent 1200 series, USA). The HPLC analysis was performed as follows. The composition of mobile phase was 71% water and 29% acetonitrile with 0.1% trifluroacetic acid. The flow rate was 1 mL/min throughout the 10-min run at 40°C. Chromatography was performed at 40°C and the eluent was monitored at a wavelength of 260 nm.

Animal study. The Institutional Animal Care and Use Committee at Asan medical center approved this study, which was conducted in accordance with the United States National Institutes of Health Guidelines on Humane Care and Use of Laboratory Animals.

Six male mongrel dogs (weight range, 20–25 kg; Orient Bio, Seongnam, Korea) were used for this study. A total of 12 NFCSs were placed in the proximal and distal urethras of six dogs.

Dogs were divided into two groups with 3 dogs each. The dogs in the control stent (CS) group received non-drug eluting NFCSs in the proximal and distal urethras and the dogs in the drug stent (DS) group received EW-7197 (1000 μg)-eluting NFCSs in the proximal and distal urethras. All dogs were maintained in an independent cage (width: 1150 mm, depth: 1430 mm, and height: 2210 mm) made of stainless steel and they were allowed to socialize with animal care staff when the cage was cleaned twice a day. All dogs were supplied with food and water and mean room temperature was kept at 24°C with a 12-hour day-night schedule, which was fully automatically controlled. After stent placement, daily diet consumption, weight change, and behavioral change were monitored on a weekly basis. At 8 weeks after stent placement, dogs were sacrificed for histologic analysis. None of the dogs died prior to the study endpoints.

Stent placement. General anesthesia was induced by intra-muscularly administered ketamine hydrochloride (Yuhan, Seoul, Korea) and atropine sulfate (Daewon, Seoul, Korea) and was maintained with intravenously administered ketamine hydrochloride. After disinfecting the external urethral orifice with 0.05% chlorhexidine (Daewoong, Seoul, Korea), the urethra was lubricated using 2% lidocaine jelly (Dongsan, Ansan, Korea). A 180-cm guide wire (Radiofocus M; Terumo, Tokyo, Japan) was then inserted through the urethra and advanced into the urinary bladder. Retrograde urethrography (RGU; Omnipaque 300; GE Healthcare, Cork, Ireland) was performed using a straight 5F graduated catheter (Cook, Bloomington, Indiana) to determine the location of stent placement. Under fluoroscopic guidance (Artis Zee Multipurpose; Siemens, Muenchen, Germany), a stent-delivery system, consisting of a 10F sheath, a guiding olive tip, and a pusher catheter, was passed over the guide wire and advanced to the middle portion of the proximal urethra. The pusher catheter was then held in place with one hand while the sheath was slowly withdrawn in a continuous motion with the other hand until the NFCS was deployed. The stent-delivery system was then removed with the guide wire left in place, and another NFCS was placed in the middle portion of the distal urethra using the same technique. Antibiotics (penicillin, 800,000 U/day) and analgesics (ketoprofen, 1 ml/5 kg) were used for a period of three days after stent placement.

Urethrographic examination. In all dogs, RGU was performed in right anterior oblique projections with use of a straight 5F graduated catheter (Cook, Bloomington, Indiana) immediately after stent placement to verify position and patency of the stent. Follow-up RGU was performed 4 and 8 weeks later, and the luminal diameter was measured with the use of calibrated catheter. Software (Photoshop, version 6.0; Adobe Systems, Palo Alto, Calif) was used to acquire digital measurements of the inner luminal diameter of the stented urethra at three different levels. Measurements were repeated three times at each level, yielding an average value per level, and these values were subsequently averaged to obtain an overall average diameter of the segment. Analyses of the urethrographic findings were performed on the basis of the consensus of three observers blinded to the study.

Histological examination. All dogs were sacrificed by means of administration of an overdose of xylazine hydrochloride (Rompun; Bayer, Seoul, Korea) 8 weeks after stent placement. The urethral tissue samples were fixed in 10% neutral-buffered formalin for 24 h. Fixed tissue samples were longitudinally sectioned at the three different portions of the segment with the stent (Fig 2). Paraffin blocks were prepared from the tissue samples and 5-μm-thick sections were obtained with a MR2258 microtome (HostoLine, Pantigliate, Italy). The slides were stained with hematoxylin and eosin (H&E) and Masson's trichrome (MT) stains. Histological examination after H&E staining included determining the degree of submucosal inflammatory cell infiltration, the number of epithelial layers, the thickness of submucosal fibrosis, and the thickness of papillary projection. The degree of inflammatory cell infiltration was subjectively determined according to the distribution and density of the inflammatory cells (graded as 1, mild; 2, mild to moderate; 3, moderate; 4, moderate to severe; and 5, severe). The average
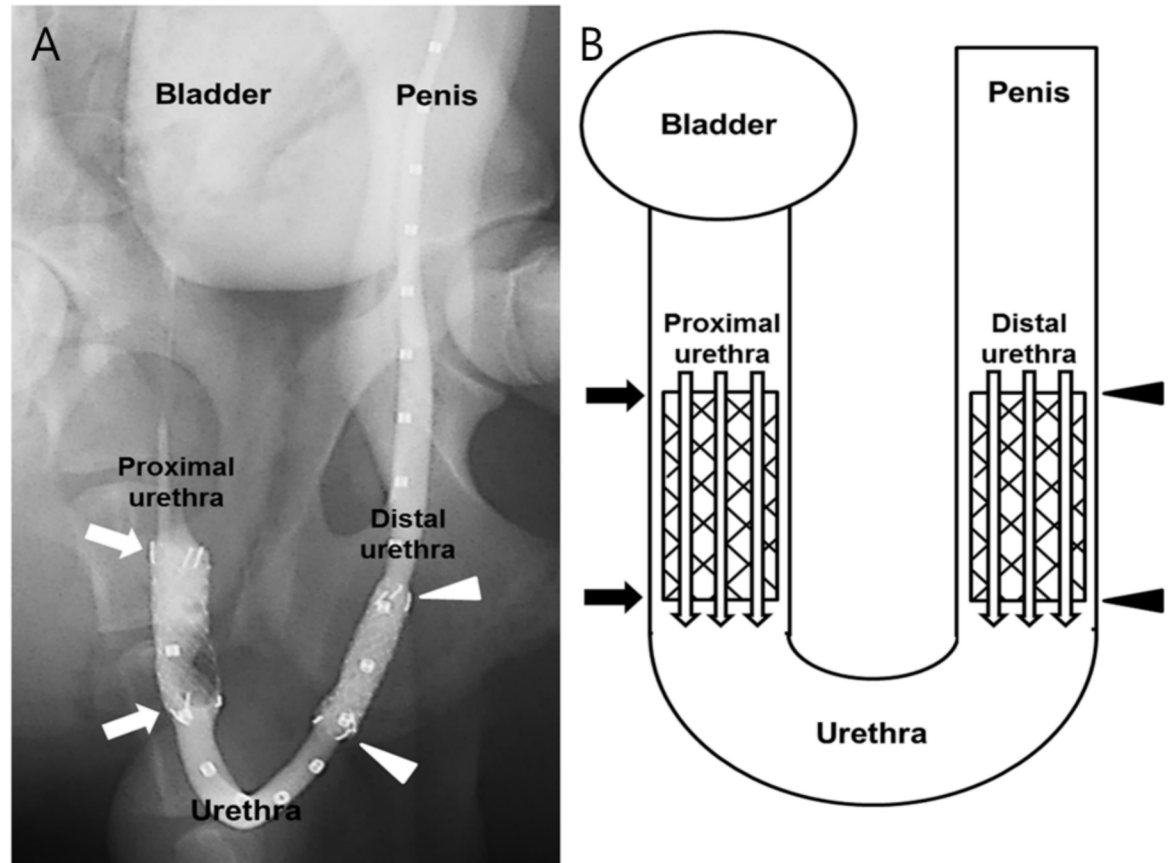
Fig 2. Locations of tissue sampled for histological examination. The canine urethra consists of the proximal pelvic urethra (arrows) and the distal cavernous urethra (arrowheads). (A) Retrograde urethrography of the canine urethra immediately after stent placement. (B) Schematic image showing the locations of tissue samples where a stent was present.

https://doi.org/10.1371/journal.pone.0192430.g002

values for the degree of inflammatory cell infiltration, the number of epithelial layers, the thickness of submucosal fibrosis, and the thickness of papillary projection were obtained by averaging eight points [18–20]. The degree of collagen deposition was determined on MT stained sections. Degree of collagen deposition was subjectively determined where 1 = mild, 2 = mild to moderate, 3 = moderate, 4 = moderate to severe, and 5 = severe. Histological examination of the urethra was performed with a BX51 microscope (Olympus, Tokyo, Japan). Measurements were obtained using Image-Pro Plus software (Media Cybernetics, Silver Spring, MD, USA). Analyses of the histological findings were performed on the basis of the consensus of three observers blinded to the study.

Statistical analysis. Data are expressed as the mean ± standard deviation. Comparisons between two groups were performed using the Mann–Whitney test. A p value of <0.05 indicates statistical significance. Statistical analyses were performed using SPSS software (version 22.0; SPSS, IBM, Chicago, IL, USA).

Results

In vitro release study

To evaluate the drug release behavior of the PU (core)—PLLLA (shell) stents, *in vitro* drug release was monitored for 60 days using an HPLC system. As shown in Fig 3, approximately
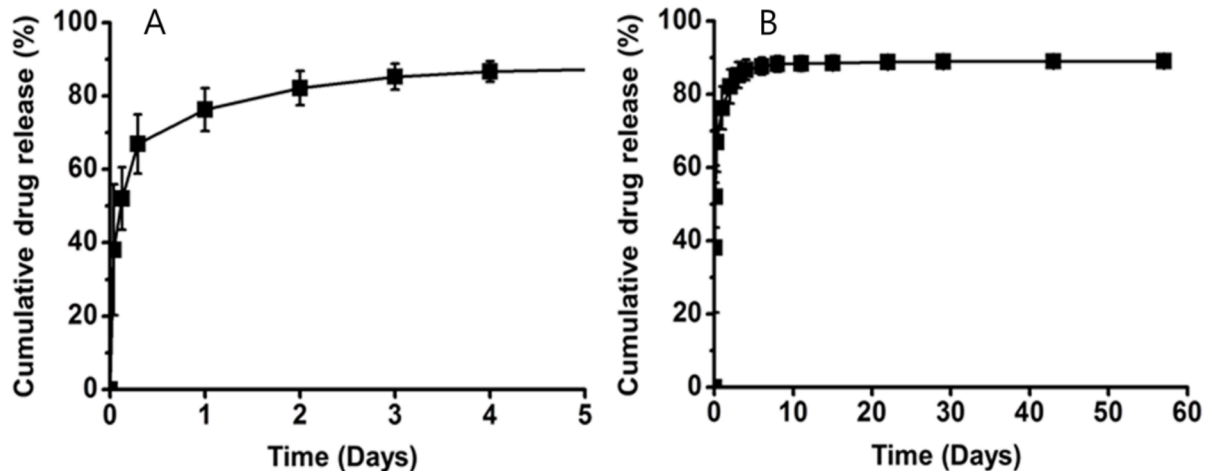
Fig 3. Curves show *in vitro* release profiles of EW-7197 from nanofiber membrane at (A) 5 days and (B) 60 days. Error bars = standard deviation of mean (n = 6).

https://doi.org/10.1371/journal.pone.0192430.g003

80% of the encapsulated EW-7197 was released from the stents within 1 day, and the remaining encapsulated EW-7197 was slowly released thereafter.

Stent placement

Stent placement was technically successful in all dogs without complications. A small amount of hematuria occurred immediately after stent placement in all dogs, but it subsided spontaneously. All animals survived until the end of the study without stent-related complications.

Urethrographic findings

The urethrographic findings are summarized in Table 1 and are presented in Fig 4. At 4 weeks, the luminal diameter of the proximal stented urethra in the DS group was significantly larger than the CS group ($p < 0.001$). There was also a significant difference between the DS and CS groups ($p = 0.002$) in the luminal diameter of the distal stented urethra. The overall luminal diameter of the stented urethra in the DS group was significantly larger than the CS group ($p < 0.001$). At 8 weeks, the luminal diameter of the stented urethra in the DS group was significantly larger than the CS group for both the proximal ($p < 0.001$) and distal urethras ($p = 0.015$).

Histological findings

The histological findings are presented in Table 2, and examples are shown in Fig 5. The overall mean thickness of the papillary projection was significantly less in the DS group than in the

Table 1. Retrograde urethrographic findings after stent placement in canine urethra.

Location	4 weeks follow-up		*p* value	8 weeks follow-up		*p* value
	CS group	DS group		CS group	DS group	
Proximal	7.36 ± 1.51	9.20 ± 1.74	<0.001	6.68 ± 1.39	8.60 ± 1.37	<0.001
Distal	6.62 ± 1.32	8.31 ± 1.57	0.002	6.20 ± 1.05	7.72 ± 1.58	0.015
Total	6.99 ± 1.45	8.67 ± 1.66	<0.001	6.51 ± 1.27	8.16 ± 1.46	<0.001

Note. Data are mean diameters of the six stented urethra in millimeters ± standard deviations. CS; control stent, DS; drug stent

https://doi.org/10.1371/journal.pone.0192430.t001
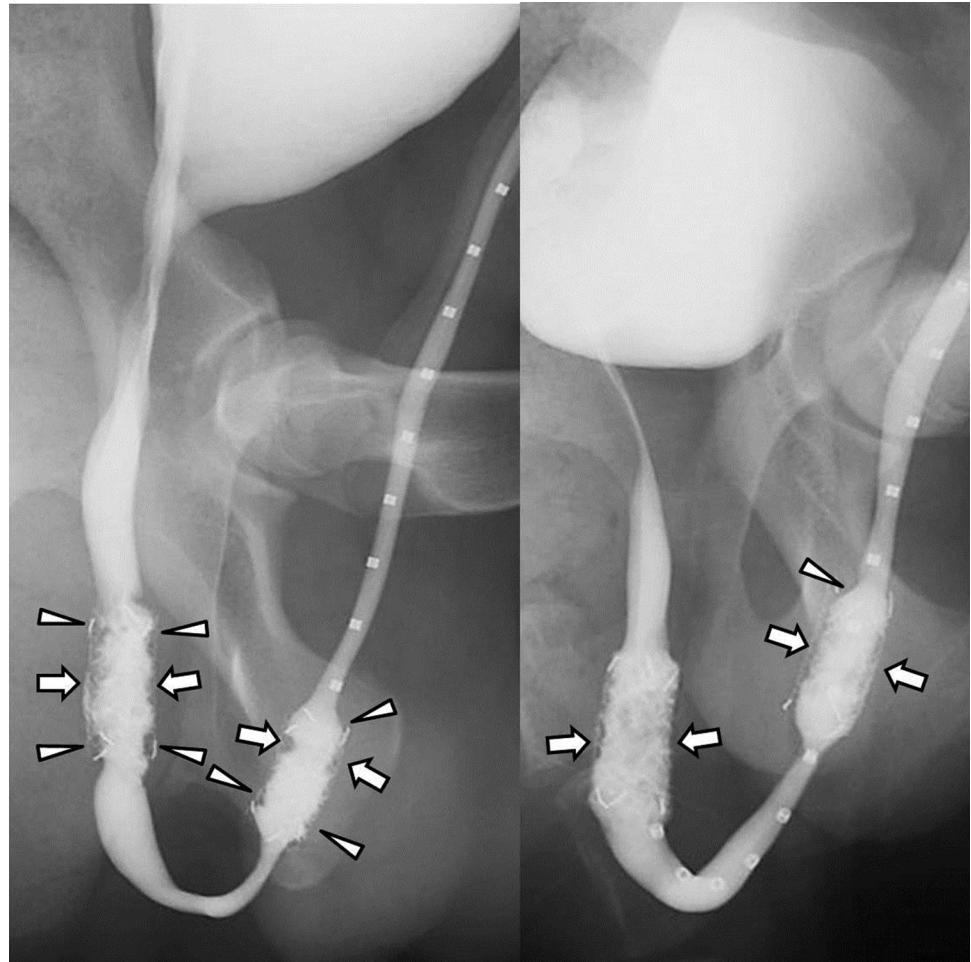
Fig 4. Retrograde urethrography images obtained 8 weeks after stent placement in dogs. (A) Image obtained after control stent placement shows filling defects (arrowheads) at both ends of the stents and in-stent stenosis (arrows) resulting from granulation tissue formation. (B) Image in drug stent group shows mild in-stent restenosis (arrows) in the proximal and distal stented urethras (arrows). At both ends of the stents, no definite filling defects were seen.

https://doi.org/10.1371/journal.pone.0192430.g004

CS group for both the proximal and distal stented urethra (all $p < 0.001$). The mean thickness of submucosal fibrosis (all $p < 0.001$) and the mean number of epithelial layers (all $p < 0.001$) were also significantly less in the DS group than in the CS group for both the proximal and distal stented urethra. The mean degree of inflammatory cell infiltration did not significantly differ between the CS and DS groups ($p = 0.480$; proximal urethra, $p = 0.484$; distal urethra, $p = 0.742$). The mean degree of collagen deposition was significantly less in the DS group than in the CS group for both the proximal and distal urethras (all $p < 0.001$). The comparison between the proximal and distal urethras did not show significant differences for any variables between groups (all $p > 0.05$).

Discussion

Placement of SEMSs for benign and malignant strictures of various organs has been around for several decades [1–5]. The downside of this treatment is restenosis resulting from granulation tissue formation through the mesh or around the edges of the stents [21]. Deeper understandings into the pathophysiology of granulation tissue formation and advances in stent

Table 2. Histological findings after stent placement in canine urethra.

	Location	CS group	DS group	*p* value
Thickness of Papillary Projection (mm)	**Proximal**	2.67 ± 0.48	1.11 ± 0.28	<0.001
	Distal	2.78 ± 0.56	1.26 ± 0.35	<0.001
	Total	2.72 ± 0.52	1.19 ± 0.31	<0.001
Thickness of Submucosal Fibrosis (mm)	**Proximal**	1.27 ± 0.55	0.67 ± 0.11	<0.001
	Distal	1.33 ± 0.64	0.64 ± 0.12	<0.001
	Total	1.30 ± 0.58	0.66 ± 0.11	<0.001
Number of Epithelial Layers	**Proximal**	4.84 ± 0.76	3.56 ± 0.72	<0.001
	Distal	5.16 ± 0.88	3.44 ± 0.72	<0.001
	Total	5.00 ± 0.83	3.50 ± 0.71	<0.001
Degree of Inflammatory Cell Infiltration	**Proximal**	3.28 ± 0.77	3.16 ± 0.72	0.506
	Distal	3.13 ± 0.66	3.06 ± 0.84	0.742
	Total	3.20 ± 0.72	3.11 ± 0.78	0.480
Degree of Collagen Deposition	**Proximal**	4.41 ± 0.67	3.34 ± 0.75	<0.001
	Distal	4.44 ± 0.62	3.44 ± 0.76	<0.001
	Total	4.42 ± 0.64	3.39 ± 0.75	<0.001

Note. Data are mean ± standard deviation. CS; control stent, DS; drug stent

technology have expanded their clinical applications. There have been several efforts to use drug-eluting stents in the treatment of strictures in nonvascular luminal organs [22–24]. The benefits of stent-based drug delivery are to maximize the level of therapeutic agents in local tissue, lower drug dosage, and minimize systemic toxicity. In the present study, we designed EW-7197-eluting covered stents and tested their efficacy in suppressing granulation tissue formation in an animal model. Our results suggest that EW-7197 locally delivered by a stent successfully reduces or inhibits granulation tissue formation secondary to stent-induced mechanical injury in a canine urethral model, as evidenced by significantly larger luminal diameter on RGU and less granulation tissue formation on histological examination in the DS group than in the CS group.

TGF-β and its receptors are uniformly overexpressed in fibrotic diseases of various organs, and it has been reported to be a potent, profibrogenic cytokine resulting in pathologic fibrosis [9,25]. Therefore, the signaling pathway for fibrosis via TGF-β has been a promising target for drug development. Various attempts to block the TGF-β pathway have been made and EW-7197 is a recently introduced TGF-β type-1 receptor kinase inhibitor [13]. The safety and efficacy of EW-7197 has been documented in animal models, and several investigators have reported that EW-7197 safely inhibited hepatic, renal, and pulmonary fibrosis and stent-induced granulation tissue formation by blocking the TGF-β/Smad and/or reactive oxygen species (ROS) signaling pathway [15,16,26]. As stent-induced benign stricture appeared to be subject to TGF-β, EW-7197 was used as an antifibrotic agent in the present study.

In the current study, granulation tissue formation based on the luminal diameter of the stented urethra and histological examination was significantly decreased in the DS group compared to the CS group in both the proximal and distal urethras. In a study by Shin et al., they placed the paclitaxel-eluting covered stents into canine urethras and reported that decreased granulation tissue formation was observed only in the proximal urethra [20]. They postulated that the distal urethra, with a smaller diameter, was less expandable and exposed to higher mechanical microtrauma than in the proximal urethra. As a result, granulation tissue formation was thought to be more prominent in the distal urethra. Despite the different anatomic
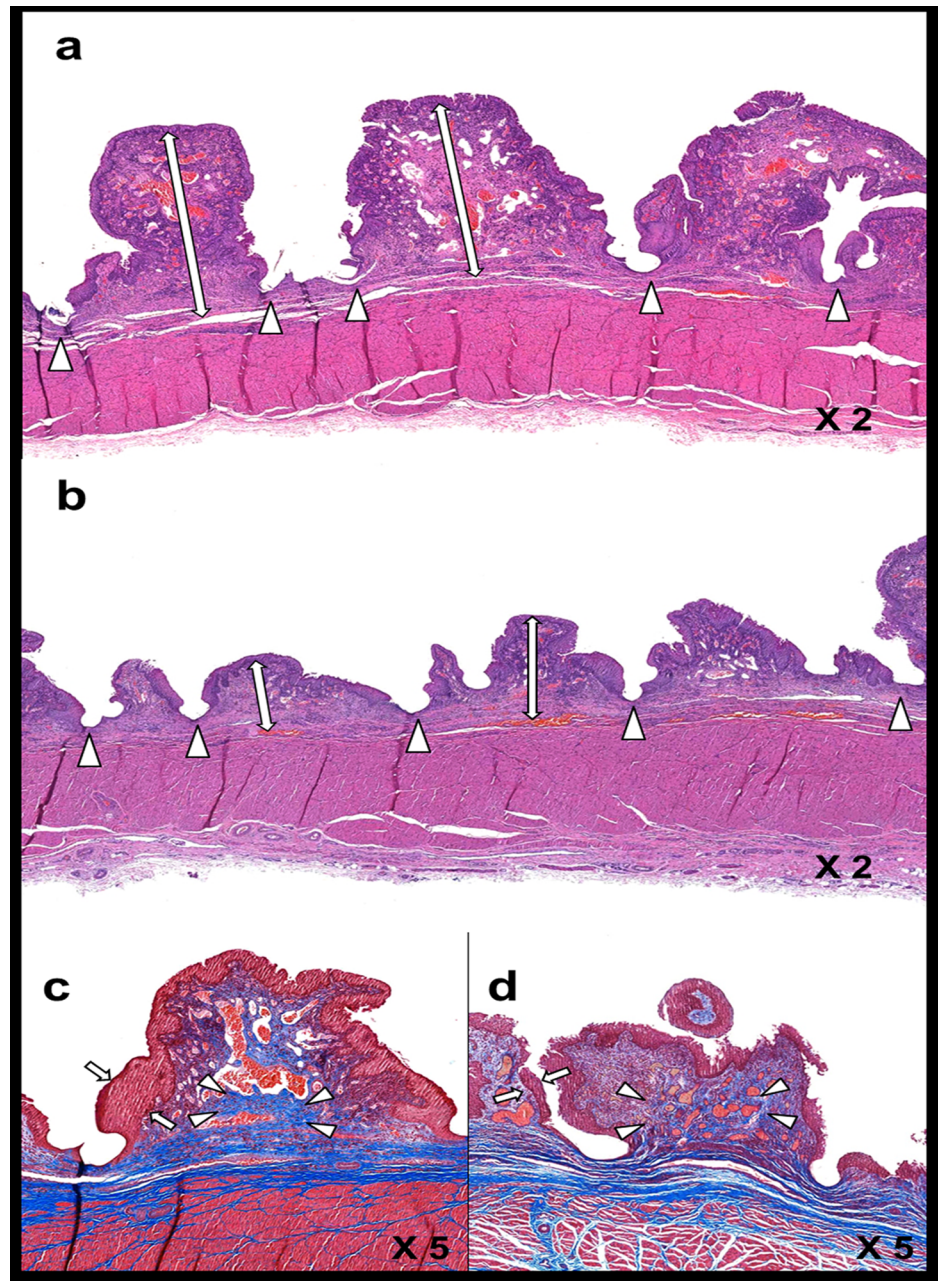
Fig 5. Representative microscopic images (hematoxylin and eosin staining magnification × 2 [A,B] and Masson's trichrome staining magnification × 5 [C,D]) of histological sections at 8 weeks after stent placement. The thickness of papillary projection (arrows) was significantly increased in the CS group (A) compared to the DS group (B). Arrowhead = stent struts (A,B). The degree of collagen deposition (arrowheads) was significantly greater in the CS group (C) than the DS group (D). The number of epithelial layers (arrows) in the CS group (C) was significantly higher than the DS group (D). CS: control stent, DS: drug stent.

https://doi.org/10.1371/journal.pone.0192430.g005

milieu between the proximal and distal urethras, granulation tissue formation was uniformly suppressed in the DS group in this study. The possible reason for the discrepancy is that EW-7197 has a more potent antifibrotic effect than paclitaxel for overcoming the harsher environment in the distal urethra.

On histological examination, the mean thicknesses of papillary projection, thickness of sub-mucosal fibrosis, number of epithelial layers, and degree of collagen deposition were significantly less in the DS group than in the CS group, whereas inflammatory cell infiltration was not different. Given the key role of TGF-β in fibrosis after stent-induced mechanical injury, a previous study demonstrated that oral administration of EW-7197 after bare metallic stent placement successfully inhibited granulation tissue formation by blocking the TGF-β signaling pathway in a rat esophageal model [15]. Although inflammatory cells may be continuously recruited by an indwelling stent acting as the stimulus, EW-7197 appears to prohibit the inflammatory phase from progressing to the proliferative phase [10]. In a study by Kim et al., they placed bare metallic stents into rat urethra and investigated the efficacy of intraperitoneal administration of IN-1233, another TGF-β type-1 receptor kinase inhibitor [27]. Their outcomes were consistent with the present study, except for inflammatory cell infiltration, which was significantly increased in the drug group in their study. EW-7197 was a newer TGF-β type-1 receptor kinase inhibitor class drug and did not seem to stimulate inflammatory cell infiltration that had been seen in IN-1233. As the accumulation of inflammatory cells may increase the likelihood of subsequent granulation tissue formation, EW-7197 is assumed to be a better candidate for drug-eluting stents.

Nanofiber coating by means of electrospinning was attempted to overcome the initial burst of the drug-eluting stents that was observed with PU-covered stents [20,22,28]. Surprisingly, the in vitro release study demonstrated that approximately 80% of the drug was eluted from the stents within 1 day after which the elution rate slowed down and reached a plateau after 10 days. This was in marked contrast to the sustained drug delivery from the NFCS in a previous report [17]. Despite the unexpected in vitro findings, our current EW-7197-eluting NFCS is able to suppress granulation tissue formation after stent placement. We have two theories for the substantial release of the drug at an early phase. As the in vitro pharmacokinetic properties of EW-7197 may differ significantly from those in in vivo settings, including the low pH of the canine urethra, there is a possibility that the excellent outcome resulted from a slower but steadier in vivo release of the drug. This hypothesis warrants further studies to see if the similar drug elution pattern can be acquired in the in vivo environment. The other assumption is that the anti-fibrogenic effect of EW-7197 was so potent that granulation tissue formation was suppressed in a prolonged fashion even with the initial burst of about 80% of EW-7197. This encourages more research on whether EW-7197 is effective in inhibiting fibrosis with 1 or 2 days of administration rather than sustained drug release.

On RGU, filling defects and luminal irregularities due to granulation tissue formation were seen at both ends of the stent as well as the stented urethra. This was likely attributable to the partial degradation of the covering membrane. The acidic environment of the urethra might have taken its toll on the PDLLA-PU complex covering membrane itself and led to the partial degradation. As the covering membrane hinders the granulation tissue from growing through the stent mesh, further studies are needed to develop a better EW-7197-eluting covering material that does not degrade.

There were some limitations in this study. First, although many of the variables of interest reached statistical significance, the sample size was too small to perform a robust statistical analysis. However, the differences in RGU and histological findings between the two groups were indisputable. Second, quantitative analyses for the expression levels of TGF-β and its mediators, such as Smad2/3, were not possible because the stents were placed in a canine urethra model. Third, we could not conduct in vivo pharmacokinetic studies on the EW-7197-eluting NFCS because of the small sample size and also did not evaluate in vitro degradation and mechanical properties of the PDLLA fibrous membranes. Given the unexpected in vitro drug release profile, in vivo pharmacokinetic studies are warranted. Third, some of the

measurements in this study were obtained subjectively and quantitative data such as morpho-metric analyses or cell counting would have provided more reliable data. Finally, long-term effectiveness of the EW-7197-eluting NFCS was not evaluated. If granulation tissue had developed after 100% of the encapsulated EW-7197 had been released, it would have provided further evidence supporting the effectiveness of EW-7197 in inhibiting stent-induced granulation tissue formation.

In conclusion, the direct and local therapy with EW-7197 via a covered stent is effective and safe for suppressing granulation tissue formation after stent placement in a canine urethral model. The promising results in this study warrant further studies on this drug for broader applications for stents in other parts of the organs.

Supporting information

S1 Table. Data of the diameter of the proximal and distal canine urethras and the micro-scopic findings in both groups after stent placement.
(XLSX)

Author Contributions

Conceptualization: Kichang Han, Su-Geun Yang, Deok Hee Lee, Ho-Young Song.

Data curation: Su-Geun Yang, Min Tae Kim.

Formal analysis: Jiaywei Tsauo, Min Tae Kim.

Funding acquisition: Deok Hee Lee, Min Tae Kim.

Investigation: Kichang Han, Dae-Kee Kim, Ho-Young Song.

Methodology: Jung-Hoon Park, Su-Geun Yang, Dae-Kee Kim, Ho-Young Song.

Project administration: Jung-Hoon Park, Kun Yung Kim.

Resources: Deok Hee Lee, Dae-Kee Kim, Dong-Hyun Kim.

Software: Jiaywei Tsauo, Sung Gwon Gang, Dong-Hyun Kim.

Supervision: Su-Geun Yang, Deok Hee Lee, Sung Gwon Gang, Dong-Hyun Kim, Ho-Young Song.

Validation: Jung-Hoon Park, Jiaywei Tsauo, Kun Yung Kim, Sung Gwon Gang.

Visualization: Jiaywei Tsauo, Sung Gwon Gang.

Writing – original draft: Kichang Han, Jung-Hoon Park.

Writing – review & editing: Kichang Han, Jung-Hoon Park.

References

1. Holm AN, de la Mora Levy JG, Gostout CJ, Topazian MD, Baron TH. Self-expanding plastic stents in treatment of benign esophageal conditions. Gastrointest Endosc. 2008; 67: 20–25.

2. Park JH, Lee JH, Song HY, Choi KD, Ryu MH, Yun SC, et al. Over-the-wire versus through-the-scope stents for the palliation of malignant gastric outlet obstruction: A retrospective comparison study. Eur Radiol. 2016; 26: 4249–4258. https://doi.org/10.1007/s00330-016-4289-3 PMID: 26984431

3. Park JH, Song HY, Kim JH, Jung HY, Kim JH, Kim SB, et al. Polytetrafluoroethylene-covered retriev-able expandable nitinol stents for malignant esophageal obstructions: factors influencing the outcome of 270 patients. AJR Am J Roentgenol. 2012; 199: 1380–1386. https://doi.org/10.2214/AJR.10.6306 PMID: 23169734

4. Song HY, Do YS, Han YM, Sung KB, Choi EK, Sohn KH, et al. Covered, expandable esophageal metal-lic stent tubes: experiences in 119 patients. Radiology. 1994; 193: 689–695. https://doi.org/10.1148/radiology.193.3.7526414 PMID: 7526414

5. Song HY, Park H, Suh TS, Ko GY, Kim TH, Kim ES, et al. Recurrent traumatic urethral strictures near the external sphincter: treatment with a covered, retrievable, expandable nitinol stent—initial results. Radiology. 2003; 226: 433–440. https://doi.org/10.1148/radiol.2262012160 PMID: 12563137

6. Culha M, Ozkuvanci U, Ciftci S, Saribacak A, Ustuner M, Yavuz U, et al. Management of recurrent bul-bar urethral stricture-a 54 patients study with Allium bulbar urethral stent (BUS). Int J Clin Exp Med. 2014; 7: 3415–3419. PMID: 25419377

7. Jordan GH, Wessells H, Secrest C, Squadrito JF Jr., McAninch JW, Levine L, et al. Effect of a tempo-rary thermo-expandable stent on urethral patency after dilation or internal urethrotomy for recurrent bul-bar urethral stricture: results from a 1-year randomized trial. J Urol. 2013; 190: 130–136. https://doi.org/10.1016/j.juro.2013.01.014 PMID: 23313208

8. Na HK, Song HY, Yeo HJ, Park JH, Kim JH, Park H, et al. Retrospective comparison of internally and externally covered retrievable stent placement for patients with benign urethral strictures caused by traumatic injury. AJR Am J Roentgenol. 2012; 198: W55–61. https://doi.org/10.2214/AJR.11.6792 PMID: 22194516

9. Karagiannidis C, Velehorschi V, Obertrifter B, Macha HN, Linder A, Freitag L. High-level expression of matrix-associated transforming growth factor-beta1 in benign airway stenosis. Chest. 2006; 129: 1298–1304. https://doi.org/10.1378/chest.129.5.1298 PMID: 16685022

10. Liu W, Wang DR, Cao YL. TGF-beta: a fibrotic factor in wound scarring and a potential target for anti-scarring gene therapy. Curr Gene Ther. 2004; 4: 123–136. PMID: 15032619

11. Miyajima A, Chen J, Lawrence C, Ledbetter S, Soslow RA, Stern J, et al. Antibody to transforming growth factor-beta ameliorates tubular apoptosis in unilateral ureteral obstruction. Kidney Int. 2000; 58: 2301–2313. https://doi.org/10.1046/j.1523-1755.2000.00414.x PMID: 11115064

12. Yata Y, Gotwals P, Koteliansky V, Rockey DC. Dose-dependent inhibition of hepatic fibrosis in mice by a TGF-beta soluble receptor: implications for antifibrotic therapy. Hepatology. 2002; 35: 1022–1030. https://doi.org/10.1053/jhep.2002.32673 PMID: 11981752

13. Jin CH, Krishnaiah M, Sreenu D, Subrahmanyam VB, Rao KS, Lee HJ, et al. Discovery of N-((4-([1,2,4] triazolo[1,5-a]pyridin-6-yl)-5-(6-methylpyridin-2-yl)-1H-imidazol-2 -yl)methyl)-2-fluoroaniline (EW-7197): a highly potent, selective, and orally bioavailable inhibitor of TGF-beta type I receptor kinase as cancer immunotherapeutic/antifibrotic agent. J Med Chem. 2014; 57: 4213–4238. https://doi.org/10.1021/jm500115w PMID: 24786585

14. Krishnaiah M, Jin CH, Sheen YY, Kim DK. Synthesis and biological evaluation of 5-(fluoro-substituted-6-methylpyridin-2-yl)-4-([1,2,4]triazolo[1,5-a]pyridin-6-yl) imidazoles as inhibitors of transforming growth factor-beta type I receptor kinase. Bioorg Med Chem Lett. 2015; 25: 5228–5231. https://doi.org/10.1016/j.bmcl.2015.09.058 PMID: 26483198

15. Jun EJ, Park JH, Tsauo J, Yang SG, Kim DK, Kim KY, et al. EW-7197, an activin-like kinase 5 inhibitor, suppresses granulation tissue after stent placement in rat esophagus. Gastrointest Endosc. 2017. 2017/02/01. https://doi.org/10.1016/j.gie.2017.01.013 PMID: 28137596

16. Park SA, Kim MJ, Park SY, Kim JS, Lee SJ, Woo HA, et al. EW-7197 inhibits hepatic, renal, and pulmo-nary fibrosis by blocking TGF-beta/Smad and ROS signaling. Cell Mol Life Sci. 2015; 72: 2023–2039. https://doi.org/10.1007/s00018-014-1798-6 PMID: 25487606

17. Park CG, Kim MH, Park M, Lee JE, Lee SH, Park J-H, et al. Polymeric nanofiber coated esophageal stent for sustained delivery of an anticancer drug. Macromolecular research. 2011; 19: 1210–1216.

18. Ko GY, Kim GC, Seo TS, Kim TH, Lim JO, Lee JH, et al. Covered, retrievable, expandable urethral niti-nol stent: feasibility study in dogs. Radiology. 2002; 223: 83–90. https://doi.org/10.1148/radiol.2231010734 PMID: 11930051

19. Park JH, Song HY, Shin JH, Kim JH, Jun EJ, Cho YC, et al. Polydioxanone biodegradable stent place-ment in a canine urethral model: analysis of inflammatory reaction and biodegradation. J Vasc Interv Radiol. 2014; 25: 1257–1264.e1251. https://doi.org/10.1016/j.jvir.2014.03.023 PMID: 24912878

20. Shin JH, Song HY, Choi CG, Yuk SH, Kim JS, Kim YM, et al. Tissue hyperplasia: influence of a pacli-taxel-eluting covered stent—preliminary study in a canine urethral model. Radiology. 2005; 234: 438–444. https://doi.org/10.1148/radiol.2342040006 PMID: 15671001

21. Choi EK, Song HY, Shin JH, Lim JO, Park H, Kim CS. Management of recurrent urethral strictures with covered retrievable expandable nitinol stents: long-term results. AJR Am J Roentgenol. 2007; 189: 1517–1522. https://doi.org/10.2214/AJR.07.2149 PMID: 18029894

22. Kim EY, Song HY, Kim JH, Fan Y, Park S, Kim DK, et al. IN-1233-eluting covered metallic stent to pre-vent hyperplasia: experimental study in a rabbit esophageal model. Radiology. 2013; 267: 396–404. https://doi.org/10.1148/radiol.12120361 PMID: 23315658

23. Kim SY, Kim M, Kim MK, Lee H, Lee DK, Lee DH, et al. Paclitaxel-eluting nanofiber-covered self-expanding nonvascular stent for palliative chemotherapy of gastrointestinal cancer and its related stenosis. Biomed Microdevices. 2014; 16: 897–904. https://doi.org/10.1007/s10544-014-9894-9 PMID: 25135441

24. Moon S, Yang SG, Na K. An acetylated polysaccharide-PTFE membrane-covered stent for the delivery of gemcitabine for treatment of gastrointestinal cancer and related stenosis. Biomaterials. 2011; 32: 3603–3610. https://doi.org/10.1016/j.biomaterials.2011.01.070 PMID: 21334742

25. Akhurst RJ, Hata A. Targeting the TGFbeta signalling pathway in disease. Nat Rev Drug Discov. 2012; 11: 790–811. https://doi.org/10.1038/nrd3810 PMID: 23000686

26. Kim MJ, Park SA, Kim CH, Park SY, Kim JS, Kim DK, et al. TGF-beta Type I Receptor Kinase Inhibitor EW-7197 Suppresses Cholestatic Liver Fibrosis by Inhibiting HIF1alpha-Induced Epithelial Mesenchymal Transition. Cell Physiol Biochem. 2016; 38: 571–588. https://doi.org/10.1159/000438651 PMID: 26845171

27. Kim JH, Song HY, Park JH, Yoon HJ, Park HG, Kim DK. IN-1233, an ALK-5 inhibitor: prevention of granulation tissue formation after bare metallic stent placement in a rat urethral model. Radiology. 2010; 255: 75–82. https://doi.org/10.1148/radiol.09090670 PMID: 20308445

28. Shin JH, Song HY, Seo TS, Yuk SH, Kim YH, Cho YM, et al. Influence of a dexamethasone-eluting covered stent on tissue reaction: an experimental study in a canine bronchial model. Eur Radiol. 2005; 15: 1241–1249. https://doi.org/10.1007/s00330-004-2564-1 PMID: 15906035